CHAPTER TWO

Geochemical characteristics of igneous rocks as petrogenetic indicators

2.1 Introduction

In Chapter 1 we noted that magmas with distinctive major element characteristics are associated with specific tectonic settings. For example, calc-alkaline series magmas are apparently associated uniquely with subduction, while low-K tholeiitic basalts are the typical products of magma generation at constructive plate margins. However, in general, the major element characteristics of primary mantle derived magmas are not particularly sensitive indicators of tectonic setting. Thus tholeiitic basalts are generated at mid-oceanic ridges but also in back-arc basins, oceanic islands, island arcs, active continental margins and continental flood basalt provinces. Fortunately, it is now well established that distinctive trace element and Sr–Nd–Pb isotopic signatures are associated with different magma generation environments, although their petrogenetic interpretation in some instances remains ambiguous (Chs. 5–12).

On the basis of the major element chemical variation diagrams discussed in Chapter 1, we established the existence of three dominant magma series, tholeiitic, calc-alkaline and alkaline. Within each of these series there is a continuous spectrum of rock types ranging from basic to acid, which appear to be genetically related. In terms of Figure 1.2 we can consider the existence of a primary magma spectrum, generated by partial melting processes within the upper mantle (Ch. 3), and a range of more differentiated (more SiO_2-rich) magmas related to the primary magmas by processes of fractional cystallization, magma mixing and crustal contamination (Ch. 4), which often occur in high-level magma chambers.

In investigating the geochemical characteristics of suites of cogenetic igneous rocks we thus have two fundamental objectives:

(a) to understand the processes involved in the petrogenesis of the primary magma spectrum (Ch. 3); and
(b) to understand the processes involved in the differentiation of the primary magma spectrum (Ch. 4).

In this chapter we shall focus our attention on ways of looking at major and trace element data for volcanic rocks graphically, in order to place constraints on petrogenetic processes. Detailed discussion of the processes responsible for the diverse compositions of terrestrial magmas is deferred until Chapters 3 and 4. Additionally, we shall consider those aspects of the radiogenic and stable isotope geochemistry of igneous rocks which may be of petrogenetic significance.

2.2 Chemical analysis of igneous rocks

A wide variety of instrumental techniques are commonly used for silicate rock analysis, permitting the determination of an extensive range of major and trace elements on a routine basis. Potts (1987) presents a comprehensive review of the various methods used, and the reader is referred to this source for further information.

X-ray fluorescence (XRF) is one of the most widely used instrumental methods for analysing rock samples for major elements (Na, Mg, Al, Si, P, K, Ca, Ti, Mn, Fe) and selected trace elements (Rb, Sr, Y, Nb, Zr, Cr, Ni, Cu, Zn, Ga, Ba, Pb, Th, U± La, Ce, Nd, Sm). Instrumental neutron activation analysis (INAA) is used for the analysis of specific trace elements (Sc, Co, Cr, Cs, Hf, Ta, Th, U) down to detection limits in the ppm and ppb range, and is especially useful for the analysis of the rare earth elements (La, Ce, Nd, Sm, Eu, Tb, Yb, Lu). Alternatively, the REE may be determined by isotope dilution mass spectrometry. Inductively coupled plasma (ICP) techniques are now being applied to the analysis of geological materials but, as yet, the number of samples in the literature analysed by this method is limited.

None of the commonly used techniques can provide analyses of H_2O and CO_2 or the ratio of Fe^{2+}/Fe^{3+} in igneous rocks. Consequently, these must be determined independently by other methods.

In the tables of analyses of igneous rocks from different tectonic settings, presented in Chapters 5–12, the analytical techniques employed have not been specified. In all cases major elements (expressed as wt. % constituent oxides) have been determined by XRF and trace elements (expressed as parts per million, or ppm) by a combination of XRF, INNA and isotope dilution. In general, analyses of H_2O, CO_2 and the Fe^{2+} / Fe^{3+} ratio are not listed, and the Fe content is expressed as total FeO or Fe_2O_3. In some XRF analyses the total volatile content is approximately expressed as the loss on ignition (LOI). When data for H_2O are given, H_2O^+ represents water present in a combined state within the rock in hydrous minerals (e.g. amphibole or biotite), whereas H_2O^- represents pore water, or that present in low-temperature alteration products (e.g. zeolites).

2.3 Chemical variation diagrams

A variation diagram is a simple display of the chemical differences and trends shown by a related suite of rocks (lavas) in which the compositional variation is a consequence of crystal–liquid fractionation processes, either partial melting or fractional crystallization. They may be plotted in terms of major elements or trace elements, or combinations of both. Variation diagrams provide a useful way of synthesizing a large volume of analytical data, which is clearly difficult to compare in table form. Additionally, they can provide the basis for the derivation of models to explain the petrogenesis of a particular suite.

A fundamental assumption in plotting variation diagrams for cogenetic suites of volcanic rocks is that they illustrate the course of chemical evolution of magmatic liquids. However, only analyses of phenocryst-poor or aphyric volcanic rocks can be

regarded as representative of actual magma compositions. Consequently, much of the scatter in variation diagrams is a result of background 'noise' introduced by using analyses of porphyritic samples. This is a particular problem for subduction-related suites (Ch. 6) which, in general, are highly porphyritic.

2.3.1 Major elements

One of the most commonly used types of variation diagram in igneous petrology is the Harker diagram (Harker 1909), in which the weight percent of a constituent oxide is plotted against wt.% SiO_2 as abscissa. This is one of a family of binary plots in which one element or oxide is plotted against another. Figure 1.1, the plot of $Na_2O + K_2O$ versus SiO_2 used to classify the members of the alkalic and sub-alkalic magma series, is a typical example. SiO_2 is chosen as abscissa as an index of differentiation, but any other element or oxide which displays a wide range of variation within the suite can be used (e.g. MgO or Zr).

In general, for suites of cogenetic igneous rocks, pairs of oxides are strongly correlated (Fig. 2.1), either positively or negatively. Such correlations or trends may be generated as a consequence of partial melting, fractional crystallization, magma mixing or crustal contamination, either individually or in combination (Chs 3 and 4). Chayes (1964) has argued that at least some negative correlations with SiO_2 are to be expected as a consequence of the constant sum effect, i.e. as SiO_2 ranges between 40 and 75% in suites of igneous rocks, the sum of all other oxides must fall from 60 to 25% as SiO_2 increases. However, Cox *et al.* (1979) argue that this effect is not significant and does not negate the usefulness of Harker diagrams as a basis for petrogenetic modelling.

Coherent trends on Harker diagrams are generally considered to represent the course of chemical evolution of magmas and are referred to as liquid lines of descent. In reality, individual members of a series are erupted in a random time sequence, suggesting that such trends are actually the average of the evolutionary trends of numerous batches of parental magma of similar composition. Additionally, in a natural system, it is highly unlikely that each batch of parental magma will be identical in composition and, consequently, the differentiation process may not be exactly the same in each case. This accounts for some of the scatter in addition to that introduced by sample heterogeneity and analytical error. In some magmatic provinces, a range of primary magma compositions may have evolved by broadly similar low-pressure fractional crystallization processes, producing a series of subparallel liquid lines of descent.

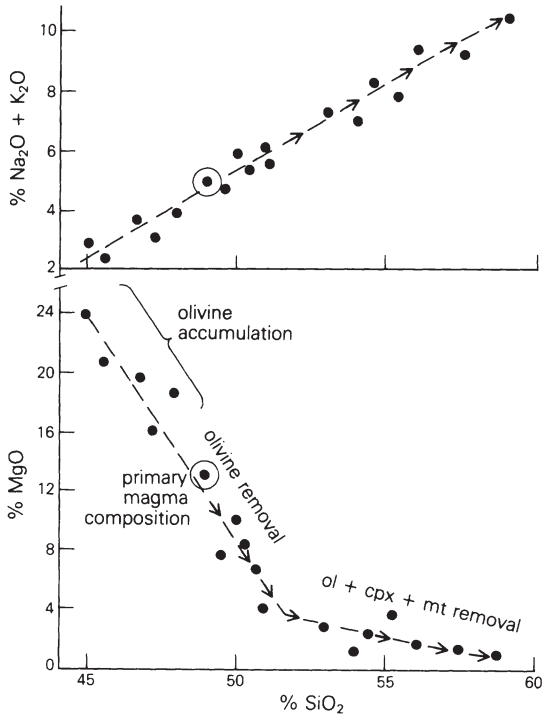

Figure 2.1 Harker variation diagrams of wt. % $Na_2O + K_2O$ and wt. % MgO versus wt. % SiO_2 for a suite of cogenetic volcanic rocks related by fractional crystallization of olivine, clinopyroxene and magnetite. The highly magnesian basalts (MgO >12%) may have accumulated olivine by crystal settling. This should be evident in their petrography, i.e. the samples should be highly olivine phyric.

Perhaps the single most important property of Harker-type variation diagrams is the applicability of the Lever Rule for mass balance (Cox *et al.* 1979). Thus it is possible to calculate graphically the way in which a liquid composition changes as a particular mineral is removed from it or a particular

contaminant is added to it. This will be considered in detail in Chapter 4. Thus if we have a suite of volcanic rocks, related by processes of fractional crystallization, which display coherent trends in several different variation diagrams, we can potentially constrain the nature of the fractionating mineral assemblage.

Variation diagrams may display strongly segmented trends (Fig. 2.2), which provides powerful evidence for the operation of crystal–liquid separation during magmatic evolution (Ch. 4). In general, the inflections in the trends are interpreted to mark the onset of crystallization of a new mineral (or group of minerals). Sometimes marked inflections are present in one two-element plot, while being undetectable in another. This is because the magnitude of the inflection is dependent on the relative positions in the diagram of the two extracts, one with the new mineral and one without it. Thus, for example, the onset of apatite crystallization may be strongly marked in a plot of P_2O_5 versus SiO_2 but not in Na_2O versus SiO_2.

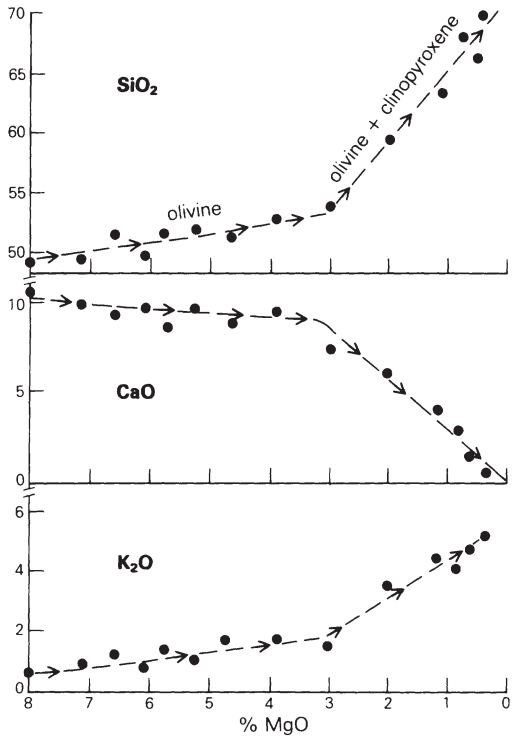

Figure 2.2 Harker-type variation diagrams, with wt.% MgO as abscissa, for a cogenetic suite of volcanic rocks related by fractional crystallization of olivine and clinopyroxene.

Another type of variation diagram employed for igneous rocks is the triangular AFM diagram (A = $Na_2O + K_2O$, F = $FeO + Fe_2O_3$, M = MgO; Fig. 1.4). This is very useful for distinguishing between tholeiitic and calc-alkaline differentiation trends in the sub-alkalic magma series.

2.3.2. Trace elements

The behaviour of trace elements during the evolution of magmas may be considered in terms of their partitioning between crystalline and liquid phases, expressed as the partition coefficient, *D*:

$$D_{xal}^{liq} = \frac{\text{concentration in mineral}}{\text{concentration in liquid}} \quad \text{for any trace element}$$

Elements that have values of $D \ll 1$ are termed *incompatible* and are preferentially concentrated in the liquid phase during melting and crystallization. Those elements which are incompatible with respect to normal mantle minerals (olivine, pyroxene, spinel and garnet; Ch. 3) are termed *lithophile* or *large-ion lithophile* (LIL), e.g. K, Rb, Sr, Ba, Zr, Th and light REE. In contrast, those with $D > 1$ (e.g. Ni, Cr) are termed *compatible*, and these are preferentially retained in the residual solids during partial melting and extracted in the crystallizing solids during fractional crystallization. Trace element partition coefficients between the major rock-forming minerals and magmatic liquids vary widely (see the Appendix). As a consequence, some elements or groups of elements may be used to identify those minerals involved in magmatic differentiation processes; these are summarized in Table 2.1.

Harker-type variation diagrams may be plotted using trace elements instead of major element oxides and may be interpreted in a similar way. Highly incompatible trace elements such as Zr may be useful as an index of differentiation if SiO_2 or MgO are inappropriate. In this section we shall concentrate on other types of trace element varia-

Table 2.1 Summary of key trace element parameters useful in evaluating petrogenetic models (after Green 1980).

Element	Interpretation
Ni, Co, Cr	High values (e.g. Ni = 250–300 ppm, Cr = 500–600 ppm) for these elements are good indicators of derivation of parental magmas from a peridotite mantle source. Decrease of Ni (and to a lesser extent Co) through a rock series suggests olivine fractionation. Decrease in Cr suggests spinel or clinopyroxene fractionation.
V, Ti	These elements show parallel behaviour in melting and crystallization processes. They are useful pointers to the fractionation of Fe–Ti oxides (ilmenite or titanomagnetite). When V and Ti show divergent behaviour, Ti substitution into some accessory phase such as sphene or rutile may be indicated.
Zr, Hf	These are classic incompatible elements, not readily substituting in major mantle phases. However, they may substitute for Ti in accessory phases such as sphene and rutile.
Ba	Substitutes for K in K-feldspar, hornblende and biotite. Changes in Ba content or K/Ba ratio may indicate the role of one of these phases.
Rb	Substitutes for K in K-feldspar, hornblende and biotite. K/Rb ratios provide possible indicators of the role of these phases in petrogenesis.
Sr	Substitutes readily for Ca in plagioclase and for K in K-feldspar. Sr or Ca/Sr ratio is a useful indicator of plagioclase involvement at shallow levels. Sr behaves more as an incompatible element under mantle conditions.
REE	Garnet and possibly hornblende readily accommodate heavy REE and so strongly fractionate light REE. Sphene has the opposite effect accommodating the light REE. Clinopyroxene fractionates the REE but only slightly. Eu is strongly fractionated into feldspars and Eu anomalies may reflect feldspar involvement.
Y	Generally behaves as an incompatible element resembling the heavy REE. It is readily accommodated in garnet and amphibole, less so in pyroxene. The presence of accessory phases such as sphene or apatite could have a major effect on the abundance of Y, since these phases readily concentrate it.

tion diagram which provide constraints for the petrogenesis of different magma types.

Rare earth elements (REE)

The rare earth elements are a group of 15 elements (La, Ce, Pr, Nd, Pm, Sm, Eu, Gd, Tb, Dy, Ho, Er, Tm, Yb, Lu) with atomic numbers ranging from 57 (La) to 71 (Lu), 14 of which occur naturally. Those with lower atomic numbers are generally referred to as light REE, those with higher atomic numbers as heavy REE, and those with intermediate atomic numbers as middle REE. They are particularly useful in petrogenetic studies of igneous rocks because all the REE are geochemically similar. All, except for Eu and Ce, are trivalent under most geological conditions. Eu is both trivalent and divalent in igneous systems, the ratio Eu^{2+} / Eu^{3+} depending upon oxygen fugacity (fO_2). Eu^{2+} is geochemically very similar to Sr. Ce may be tetravalent under highly oxidizing conditions.

In order to compare REE abundances for different rocks graphically, it is necessary to eliminate the Oddo-Harkins effect, which is the existence of higher concentrations of those elements with even atomic numbers as compared to those with odd atomic numbers. This is achieved by normalizing the concentrations of individual REE in a rock to their abundances in chondritic meteorites (Nakamura 1974). This smooths out the concentration

variations from element to element. Chondrites are used in the normalization procedure because they are primitive solar system material which may have been parental to the Earth. Fig. 2.3 shows a range of chondrite-normalized REE patterns for basaltic rocks.

Particular minerals will have a characteristic effect upon the shape of the REE pattern of the melt during partial melting and fractional crystallization,

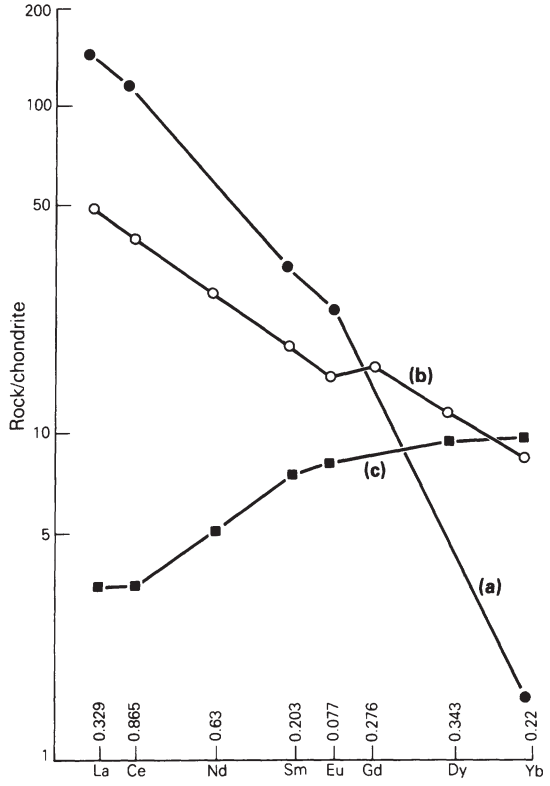

Figure 2.3 Schematic chondrite-normalized REE patterns for basaltic rocks. Normalization constants from Nakamura (1974) are indicated on the diagram. (a) Strongly light-REE enriched basalt with very low concentrations of heavy REE suggests the presence of residual garnet in the source: extremely high concentrations of light REE suggest very small degrees of partial melting or a light-REE enriched source. (b) Basalt with a slight negative Eu anomaly which may have fractionally crystallized plagioclase or may have been in equilibrium with a plagioclase-bearing mantle source: heavy-REE concentrations of $\sim$ 10 × chondritic suggest that garnet is absent from the source. (c) Basalt showing strong light-REE depletion, suggesting derivation from a light-REE depleted garnet-free source.

depending upon their D values (see the Appendix), which allows identification of their role in magmatic differentiation processes. The magnitude of the effect produced by a particular mineral will depend upon its relative abundance and on the magnitude of its D value for a particular element. Feldspars have low D's for all of the REE except Eu. Consequently, feldspar has a minor effect on the REE pattern of the melt except for the production of a negative Eu anomaly as a consequence of the high D value for Eu. The size of the Eu anomaly decreases with increasing fO_2 and temperature, but is probably significant in all magmatic systems (Hanson 1980). Garnet has very low D values for the light REE and increasingly larger D's for the heavy REE. Thus its presence in equilibrium with a magma leads to a depletion of heavy REE. Orthopyroxene and Ca-rich clinopyroxene generally have $D < 1$, with values for the light REE that are slightly lower than for the heavier, which may lead to light REE enrichment in the melt. Olivine D values for REE are all less than 0.1, and thus its presence leads to essentially equivalent enrichment for all the REE. D's for hornblende show a strong dependence on composition and may be greater than 10 for the middle REE in silica-rich systems. Thus the fractional crystallization of hornblende from intermediate-composition magmas may lead to the relative depletion of the middle REE. In contrast, biotite has generally low D's for the REE and its presence should have relatively little effect on the REE pattern of the melt. In evolved liquid compositions, zircon, apatite and sphene may strongly fractionate the REE (Le Marchand *et al.* 1987).

If the Earth originally had chondritic abundances of the REE and then differentiated to form the early mantle and the core, then the mantle would have retained the REE because they are lithophile. This would result in a primordial mantle with greater abundances of the REE (perhaps 2 to 3 times chondritic), but with a parallel pattern relative to chondrites. Partial melting of the mantle to form basalt results in a relative depletion of the light REE in the residuum, and therefore the mantle should have become progressively depleted in light REE over the course of geological time. During

partial melting the presence of residual garnet in the source leads to less enrichment of the heavy REE in the magma relative to melts derived from garnet-free mantle sources. However, even in garnet-bearing sources, once the degree of partial melting is sufficiently high to eliminate garnet from the residue (Ch. 3) fractionation of the light and heavy REE is suppressed and the REE pattern of the melt becomes subparallel to that of the source. Thus, for relatively large degrees of partial melting, we may consider that the ratios of light REE in a magma should essentially be similar to those in the source. For common mantle mineralogies (olivine, orthopyroxene, clinopyroxene, garnet and spinel) there is no phase which preferentially concentrates light REE relative to the heavy. Thus we may deduce that magmas such as the basalt 'c' in Fig. 2.3, whch display light-REE depleted patterns, must be derived from mantle sources which are themselves depleted in light REE.

In terms of Fig. 2.3, the degree of enrichment for a particular REE relative to chondritic abundances is a function of the initial concentration of that element in the source and the degree of partial melting (Ch. 3), and subsequent fractional crystallization (Ch. 4).

Spiderdiagrams

In order to understand the pattern of trace element abundances in basalts (or indeed any igneous rock) it is useful to have a reference frame to which the elemental abundances in a particular rock can be compared. We have already used this approach in the previous section by plotting chondrite-normalized REE patterns. Developing this idea further leads us to the concept of spiderdiagrams (Wood *et al.* 1979, Sun 1980, Thompson 1982, Thompson *et al.* 1984), in which the abundances of a range of incompatible trace elements are normalized to estimates of their abundances in the primordial Earth.

The elements Ba, Sr, U, Th, Zr, Nb, Ti and REE are believed to have condensed at high temperatures from a gas of solar composition during planetary formation. Archaean high-MgO basalts (komatiites) have the same ratios of these elements (e.g. Ba/Sr, U/Th) as chondritic meteorites, suggesting that their ratios in meteorites may approximate those in the primordial mantle before significant crust formation. However, while the absolute abundances of these elements in the bulk Earth may approximate to chondritic values, those in the primordial mantle may be greater due to the concentration effects of core formation.

Several variants of the spiderdiagram plot have been used in the literature, in which the order of the elements plotted varies slightly, and different normalization constants have been adopted. For example, Wood *et al.* (1979) normalize to a hypothetical primordial mantle composition, whereas Thompson *et al.* (1984) and Sun (1980) normalize their data to chondritic abundances, with the exception of K and Rb, which may be volatile during planetary formation, and P, which may be partly contained in the core. In subsequent chapters both Sun (1980) and Thompson *et al.* (1984) spiderdiagram plots have been used to discuss the trace element geochemistry of basaltic magmas formed in different tectonic settings. These diagrams are essentially identical to each other (Fig. 2.4) except for the order of some of the elements. This is somewhat arbitrary, being designed to give a smooth pattern for average MORB (Sun 1980). It is probably one of increasing incompatibility of the elements from right to left in a four-phase lherzolite (Ch. 3) undergoing partial fusion. The elements plotted all behave incompatibly ($D < 1$) during most partial melting and fractional crystallization processes. The main exceptions to this are Sr, which may be compatible with plagioclase, Y and Yb with garnet, and Ti with magnetite. Following Thompson *et al.* (1984), we shall refer to the individual patterns as spiderdiagrams.

Analytical error may be the source of many apparently spurious inflections in spiderdiagram patterns. However, once these effects have been taken into consideration, the peaks, troughs, slopes and curvature of the patterns may provide invaluable petrogenetic information concerning crystal–liquid equilibria. For example, troughs at Sr probably result from the fractional crystallization of plagioclase from many basalts. In contrast, a trough at Th and Rb combined with one at Nb–Ta may suggest contamination of a magma by lower

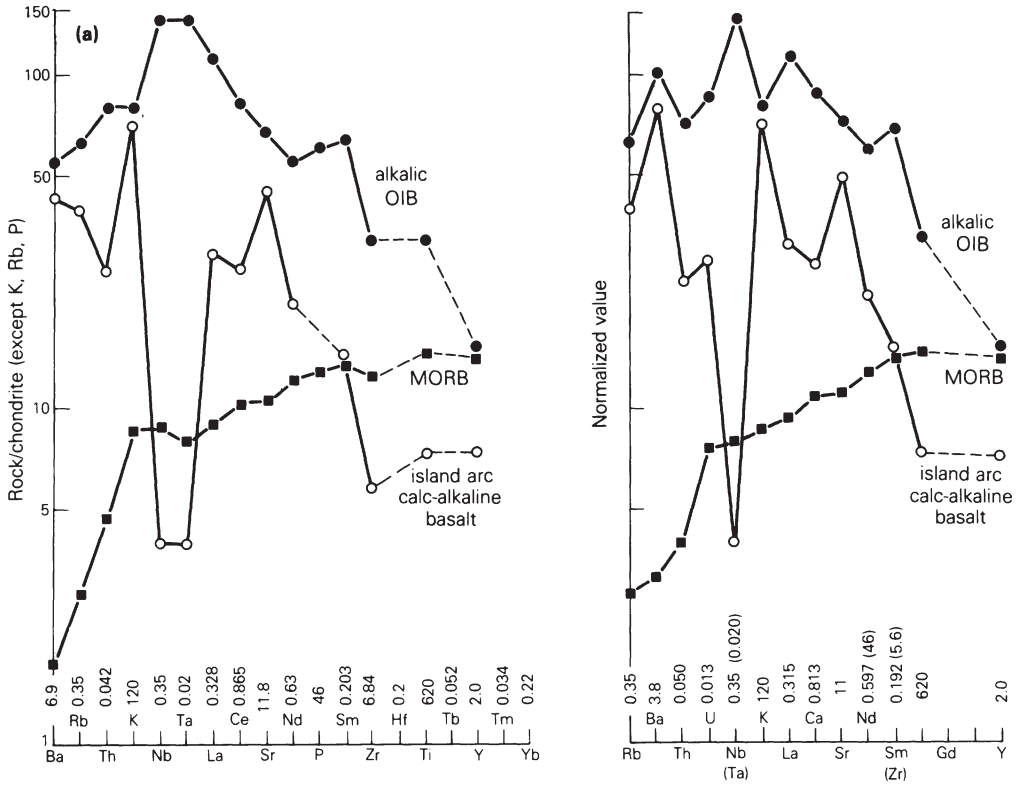

Figure 2.4 Typical spiderdiagram patterns for mid-ocean ridge (MORB), oceanic-island (OIB) and island-arc, basalts normalized according to (a) Thompson *et al.* (1984) and (b) Sun (1980). Values of the normalization constants used are given at the foot of each diagram.

continental crustal rocks (Ch. 4). The marked trough in the spiderdiagrams of some ultrapotassic intracontinental plate lavas (Ch. 12) may reflect residual phlogopite in the source.

Spiderdiagram patterns for typical mid-ocean ridge, island-arc and oceanic-island basalts are shown in Figure 2.4. MORB (Ch. 5) are considered to be the products of relatively large degrees of partial melting, and consequently their trace element patterns should reflect those of their mantle source. In general, the less incompatible elements on the right-hand side of the spiderdiagram pattern should be less enriched during partial melting, tilting the curve up to the left. Additionally, fractional crystallization subsequent to magma segregation should tilt the patterns even further up to the left. There is no known mechanism for tilting the curve down to the left, as shown, during the type of partial melting capable of creating the very large volumes of magma erupted at mid-oceanic ridges (Norry & Fitton 1983). Thus the source of MORB must clearly be depleted in the more incompatible elements such as K and Rb and, to a lesser extent, Nb and La. It has been argued that this depletion has been accomplished by the formation of the continental crust throughout geological time.

In contrast to the MORB spiderdiagram pattern, that for an alkalic oceanic-island basalt (OIB) shows extreme degrees of incompatible element enrichment with a peak at Nb–Ta, suggesting that the source may also be enriched in incompatible elements (Ch. 9). In general, the spiderdiagrams of all magnesian OIB (both tholeiitic and alkalic) approximate to smooth convex curves (Thompson *et al.* 1984).

Compared to the relatively smooth shapes of the MORB and OIB spiderdiagrams, that of the subduction-related basalt is strongly spiked. As we shall see in Chapter 6, the positive spikes are mostly a consequence of components added to the mantle source of the basalts by subduction-zone fluids. The most persistent feature of the spiderdiagrams of volcanic-arc basalts is the marked Nb–Ta trough, which has been explained in terms of retention of these elements in the source during partial melting. However, a similar trough is also a typical feature of the spiderdiagram patterns of basalts which have experienced crustal contamination (Ch. 4), and therefore an element of caution must be exercised when interpreting these sorts of patterns.

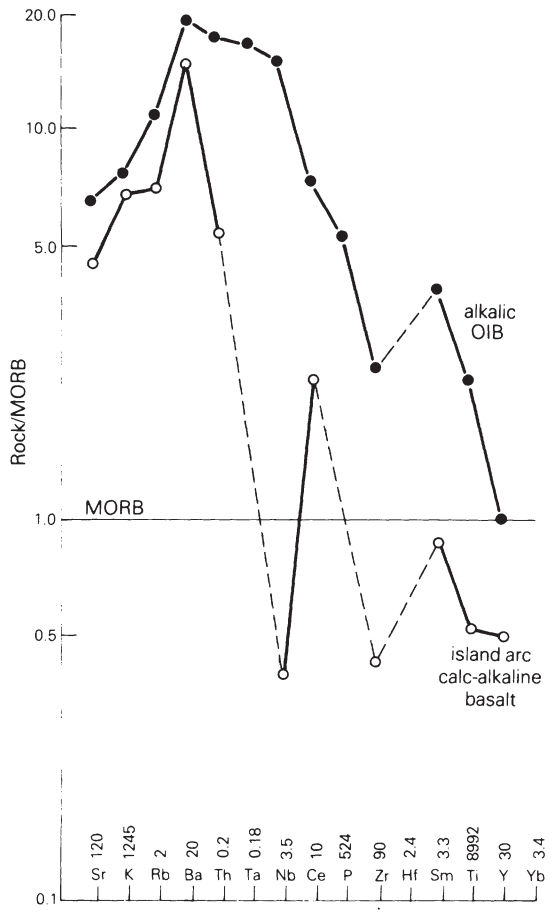

Figure 2.5 MORB-normalized trace element variation diagram for typical island-arc and oceanic-island basalts. The order of the elements and values of the normalizing constants are from Pearce (1983).

A modified version of the spiderdiagram is most useful for comparing the trace element characteristics of different types of basalts. For example, if we wish to know how continental tholeiites differ from their oceanic counterparts we could normalize their compositions to those of typical MORB or oceanic-island tholeiites. The sequence of elements plotted may be the same as that in a conventional spiderdiagram, or different (e.g. Pearce 1983). Figure 2.5 shows the island-arc and oceanic-island basalts from Figure 2.4 normalized to values in an average MORB. In this type of diagram (after Pearce op. cit.) the elements are divided into two groups based on their relative mobility in aqueous fluids. Sr, K, Rb and Ba are mobile and plot at the left of the pattern, while the remaining elements are immobile. The elements are arranged such that the incompatibility of the mobile and immobile elements increases from the outside to the centre of the pattern. Pearce considers that the shape of these patterns is not likely to be greatly changed by fractional crystallization or variable degrees of partial melting, and that they may consequently be used to discuss source characteristics. Such MORB-normalized trace element variation diagrams have been used to constrain the nature of the mantle source of subduction-related basalts (Chs 6 & 7) and continental flood basalts (Ch. 10), and the reader is referred to the appropriate sections of these chapters for a more detailed discussion of their interpretation (Sections 6.11.2 & 7.7.3).

2.4 Geochemical characteristics of primary magmas

Primary magmas are those formed by partial melting of the upper mantle, the compositions of which have not been modified subsequently by differentiation processes (fractional crystallization, crustal contamination, magma mixing, liquid immiscibility and volatile loss; see Ch. 4). As we have seen in Chapter 1, such magmas encompass a variety of types including tholeiitic, calc-alkaline and alkaline basalts. Clearly, it is of great petro-

genetic significance to be able to recognize primary magma compositions as these are parental, giving rise through differentiation processes to more evolved (more silica-rich) magma types. Unfortunately, there are no generally accepted criteria which can be used to distinguish them unequivocally from those basaltic magmas with compositions that have been modified subsequent to segregation.

O'Hara (1968) considers that most of the basaltic lavas erupted at the Earth's surface are not primary and have evolved by fractional crystallization of olivine (Ch. 4) from more MgO-rich picritic precursors. The rarity of erupted high-MgO liquids has been used to argue against this, although various authors have suggested that such liquids would be difficult to erupt by virtue of their high density. As a consequence, we generally consider that the most primitive basalts of a particular suite are those with the highest MgO contents. These may actually be parental to the suite of lavas but need not necessarily be primary. Clearly, it is much easier to demonstrate the parental nature of a magma than to confirm its primary nature.

As olivine and orthopyroxene are the most abundant minerals in the upper mantle source rocks (Ch. 3), primary magmas must be in equilibrium with these phases at their depth of segregation, and should therefore crystallize them at the liquidus in melting experiments at the appropriate pressure (Yoder 1976, Basaltic Volcanism Study Project 1981; and see Ch. 3). Additionally, the Fe^{2+}/Mg ratios of primary magmas should lie within the range expected for liquids in equilibrium with typical upper mantle olivine compositions (Fo_{86-90}). Roeder & Emslie (1970) showed that the distribution of Fe and Mg between olivine and coexisting melt, as defined by the relation:

$$K_D = (Fe^{2+}/Mg)_{olivine}/(Fe^{2+}/Mg)_{melt}$$

is relatively insensitive to temperature, melt composition and oxygen fugacity, with a K_D value of 0.3 ± 0.03. Consequently, the Mg′ values ($Mg/(Mg + Fe^{2+})$) of basalts in equilibrium with mantle olivine compositions can be calculated, and lie in the range 0.68–0.75. In general, the Mg′ value is insensitive to the degree of partial melting but is highly sensitive to the amount of subsequent fractional crystallization, particularly of olivine.

The partitioning of the trace element Ni between olivine and melt has similarly been used to constrain the compositions of primary mantle derived magmas (Ch. 3). Estimated Ni contents are relatively insensitive to the degree of partial melting and range between 400 and 500 ppm, depending upon the assumptions made about mantle mineralogy and Ni content and on the choice of values for Ni partition coefficients. Similar estimates may be made of the Cr contents of primary magmas.

In general, primary magmas in equilibrium with typical upper mantle mineralogies (olivine + orthopyroxene + clinopyroxene ± garnet ± spinel) should have high Mg′ values (>0.7), high Ni (>400–500 ppm), high Cr (>1000 ppm) and SiO_2 not exceeding 50%. However, if they are not derived from normal mantle but from metasomatized source regions (Chs 3, 6, 7, 11 & 12) these criteria may no longer be applicable. The meta somatism of the source may be so extreme that harzburgite (olivine + orthopyroxene) is no longer the residue from partial melting (Ch. 3), and thus these phases do not buffer the Mg′ values, Ni and Cr contents of the partial melts. In the absence of the above criteria the presence of high-pressure mantle-derived ultramafic xenoliths may be used to infer relatively primary characteristics for the host magma, as these would be expected to settle out if significant fractional crystallization had occurred. However, even this is not completely diagnostic, as high-pressure olivine fractionation could have occurred before incorporation of the xenoliths into the magma.

2.5 Isotopes as petrogenetic indicators

Isotope geochemical studies are now regarded as a fundamental part of the petrogenetic interpretation of igneous rocks. They are based on two groups of isotopes, radiogenic and stable. In the former, isotopic variations are caused by the radioactive decay of elements, whereas in the latter they are the consequence of mass fractionation in chemical reactions. In general, mass fractionation effects are

comparatively small, except for the lighter elements, O, H, C and S.

The naturally occurring long lived radioactive decay schemes of K, Rb, Sm, Th and U are critically important in establishing the chronology of magmatic events. The isochron method for dating co-magmatic suites of igneous rocks, which may be applied to all of these decay schemes, depends upon the fact that in a given sample the rate of accumulation of the radiogenic daughter isotope, relative to a non-radiogenic isotope of the same element, is related to the concentration ratio of the parent and daughter elements, and to the decay constant of the parent element. The dating of igneous rocks is a complex subject and the reader is referred to Faure (1986) for a detailed discussion. In the context of this chapter we shall focus our attention on the radiogenic daughters of Rb, Sm, U and Th as petrogenetic tracers in evaluating the evolution of magmas.

The importance of radiogenic isotopic variations is that they frequently survive the chemical fractionation events which accompany the formation and evolution of magmas, as isotopes of the heavier elements are not separated from each other through crystal–liquid equilibria. Thus, during partial melting, a magma will inherit the isotopic composition of its source, and this will remain constant during subsequent fractional crystallization processes, provided that the magma does not become contaminated by interaction with isotopically distinct wall rocks or other batches of magma (Ch. 4). As a consequence, estimates of the present-day isotopic characteristics of the mantle source region of basaltic magmas may be obtained from studies of young oceanic volcanic rocks (MORB and OIB), which have not been significantly contaminated by crustal rocks en route to the surface.

In general, rocks of the continental crust have very different radiogenic and stable isotope compositions from those of the mantle, and thus isotopic studies can provide important constraints on the extent of crustal contamination in lavas erupted in continental-plate tectonic settings (Ch. 4). Despite the fact that stable isotopes may become fractionated by crystal–liquid differentiation processes, the magnitude of these effects is small compared to the difference in isotopic composition between crustal and mantle reservoirs. As a consequence, oxygen isotope studies have been extensively used to assess the importance of crustal contamination effects in continental volcanic suites.

Isotopes of the rare gases, particularly He, have proved to be useful tracers of the role of primordial mantle components in the petrogenesis of oceanic-island basalts (Ch. 9). Additionally, cosmogenic radionuclides such as ^{10}Be are important as potential tracers of the role of subducted sediment in island-arc and active continental margin magmatism (Ch. 6 & 7).

In many of the provinces discussed in Chapters 5–12, the volcanic rocks are so young that their present-day radiogenic isotope ratios are identical to those at the time of their formation. Clearly, for older rocks, the isotopic compositions must always be age-corrected, as it is only the initial isotopic ratios which are directly of petrogenetic significance.

2.5.1 Radiogenic isotopes

Rb–Sr

Rb has two naturally occurring isotopes, ^{85}Rb and ^{87}Rb, of which ^{87}Rb is radioactive and decays to stable ^{87}Sr by beta emission. Sr has four naturally occurring isotopes, ^{88}Sr, ^{87}Sr, ^{86}Sr and ^{84}Sr. The precise isotopic composition of Sr in a rock or mineral that contains Rb depends upon its age and Rb/Sr ratio. This forms the basis of the Rb–Sr dating technique, using the following equation:

$$\frac{^{87}Sr}{^{86}Sr} = \left(\frac{^{87}Sr}{^{86}Sr}\right)_{initial} + \frac{^{87}Rb}{^{86}Sr}(e^{\lambda t} - 1)$$

where λ is the decay constant of $^{87}Rb(= 1.42 \times 10^{-11}yr^{-1})$ and t is the age in years.

During fractional crystallization of basaltic magma, Sr tends to be concentrated in plagioclase whereas Rb remains in the residual magma. Consequently, the Rb/Sr ratio of the magma increases gradually during the course of progressive crystallization. Thus a suite of cogenetic igneous rocks, related by processes of fractional crystallization to a

parent magma, will tend to have increasing Rb/Sr ratios with increasing degree of differention. However, provided that the system has remained closed, all members of the suite should have identical initial ratios, although they will have different present-day ratios depending upon their age and Rb/Sr ratio.

It is generally agreed upon that the matter which accreted from the solar nebula to form the proto-planet Earth had a relatively uniform $^{87}Sr/^{86}Sr$ ratio, which we refer to as the primordial value. Since accretion, the isotopic composition of Sr in the Earth has become increasingly heterogeneous as a consequence of the geochemical differentiation of the planet. Unfortunately, it is not possible to measure the isotopic composition of the Sr that was incorporated into the Earth at the time of its formation, as rocks formed at this time are either inaccessible, being located deep within the mantle, or have been destroyed by subsequent geological processes. As a consequence, we must rely on the study of meteorites and lunar samples to determine the primordial $^{87}Sr/^{86}Sr$. The value of the initial $^{87}Sr/^{86}Sr$ ratio of basaltic achondrite meteorites (BABI) (*B*asaltic *A*chondrite *B*est *I*nitial), 0.69897 ± 0.00003, is consequently taken to be that of the solar nebula at a very early stage in the formation of the planet. Thus we can consider that the Earth formed 4.5 ± 0.1 Ga ago with an $^{87}Sr/^{86}Sr$ ratio of approximately 0.699.

Crustal rocks of granitic composition, enriched in Rb relative to Sr, began to form at a very early stage in the history of the Earth and have played a dominant role in the isotopic evolution of Sr. Such materials, evolving with high Rb/Sr ratios, have developed much higher present-day $^{87}Sr/^{86}Sr$ ratios than the upper mantle, which has evolved with a very much lower Rb/Sr (Fig. 2.6). This difference is fundamental to petrogenetic studies of igneous rocks, as it enables us to trace the effects of continental crustal contamination of mantle-derived magmas. However, to do this we must know the range of $^{87}Sr/^{86}Sr$ ratios that characterize crustal materials, in addition to understanding the isotopic evoluation of Sr in the mantle throughout the course of geological time.

The present-day isotopic composition of Sr in the

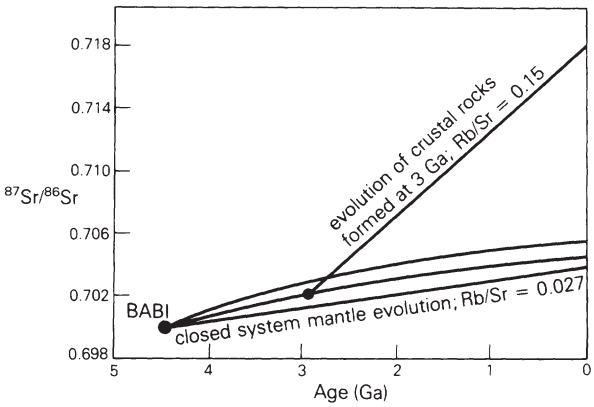

Figure 2.6 The isotopic evolution of terrestrial Sr. The curved lines represent the hypothetical evolution of Sr in the mantle from the primordial value (BABI) at 4.5 Ga to the present day. The curvature of these lines implies a time-dependent decrease in the bulk Rb/Sr ratio of the mantle. The straight line represents the closed system evolution of mantle material with an Rb/Sr ratio of 0.027.

mantle can be deduced from studies of young oceanic basalts from mid-oceanic ridges and oceanic islands, which clearly could not have been contaminated by continental crustal rocks en route to the surface. Such magmas could have assimilated oceanic crustal rocks, but as these are composed of similar materials, perhaps modified by seawater interaction, the effects will not in general be great. Figure 2.7a clearly demonstrates the considerable heterogeneity of $^{87}Sr/^{86}Sr$ in oceanic basalts, which suggests that the Rb/Sr ratio of the mantle is variable. If the Earth had evolved as a closed system with a constant Rb/Sr ratio of 0.027 to the present day, it would have an $^{87}Sr/^{86}Sr$ ratio of only 0.7040. In those regions of the mantle which have been depleted by the extraction of partial melts the Rb/Sr ratio will have been decreased, whereas in others it may have been increased as a consequence of metasomatic enrichment processes, involving the migration of incompatible element enriched fluids or partial melts. As a consequence of the differentiation of the mantle to form the rocks of the continental crust, its bulk Rb/Sr may have decreased with time.

The isotopic composition of Sr in the continental crust is markedly heterogeneous, as shown in

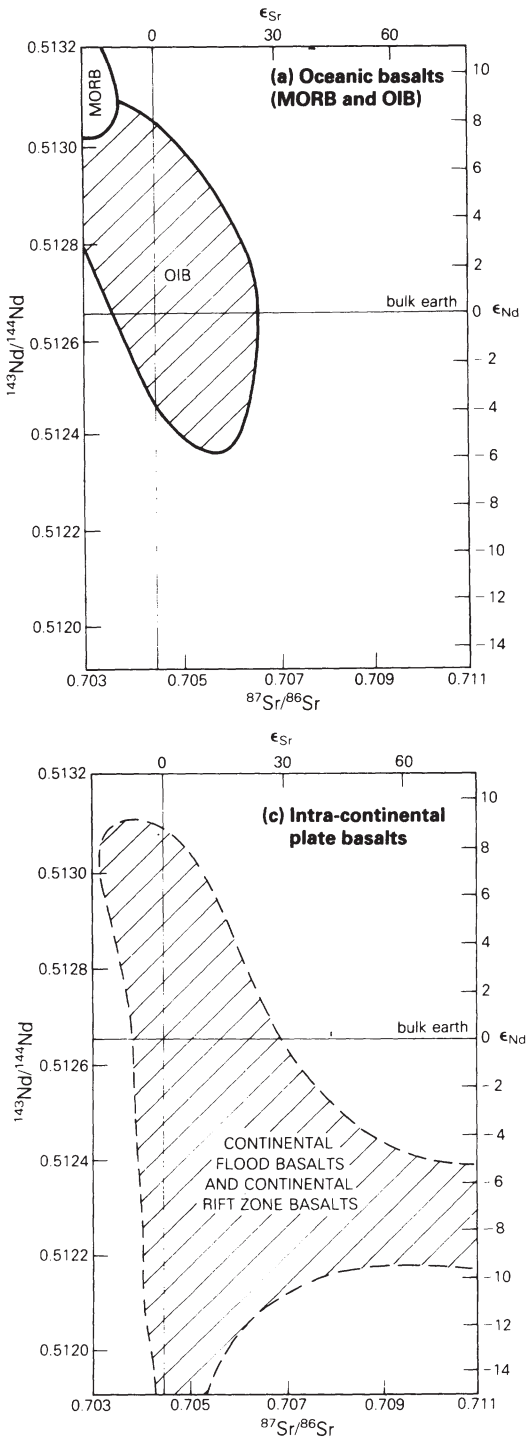

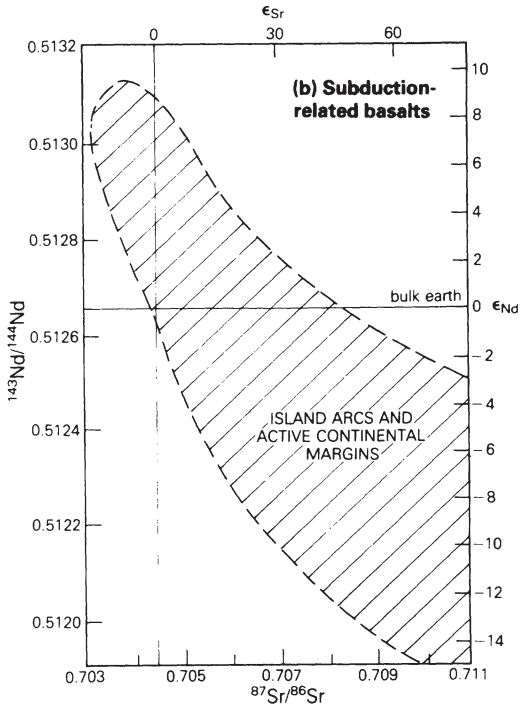

Figure 2.7 The variation of $^{143}Nd/^{144}Nd$ versus $^{87}Sr/^{86}Sr$ for volcanic rocks from different tectonic settings.

Figure 2.8, as a consequence of the wide age range and Rb/Sr ratios of crustal rocks. In general, the $^{87}Sr/^{86}Sr$ ratios are much higher than those of the upper mantle, as exemplified by the oceanic basalt array (Fig. 2.7a). Clearly, basaltic magmas erupted through the continental crust may interact with $^{87}Sr/^{86}Sr$-rich basement rocks and, as a consequence, their isotopic compositions cannot be unambiguously attributed to source mantle characteristics.

The initial isotopic composition of Sr in volcanic rocks at the time of their formation can provide important information about the mantle sources from which the magmas originate, and the processes by which their chemical and isotopic compositions may be subsequently modified during ascent to the surface. In terms of Figure 2.7, we can clearly see that there are systematic differences in the $^{87}Sr/^{86}Sr$ ratios of volcanic rocks formed in different tectonic settings, implying that the upper mantle is isotopically heterogeneous on a large scale. The lowest $^{87}Sr/^{86}Sr$ ratios occur in mid-oceanic ridge basalts (MORB), while those of oceanic-island basalts (OIB) are in general signifi-

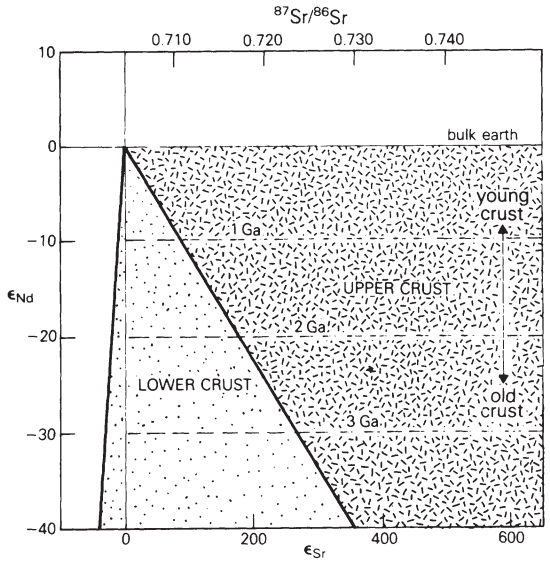

Figure 2.8 The Nd and Sr isotopic composition of continental crustal rocks at the present day; contours show the relative age of the crustal rocks in Ga (after DePaolo & Wasserburg 1979).

cantly higher. If we consider basalts generated in subduction-related and intracontinental plate-tectonic settings (Fig. 2.7b,c) an even greater range of $^{87}Sr/^{86}Sr$ ratios exists, some of which may be a consequence of continental crustal contamination. The high $^{87}Sr/^{86}Sr$ ratios of island-arc volcanic rocks (Ch. 6) have been variously attributed to the involvement of subducted sediments or sea water or, in some cases, to contamination of the magmas by interaction with terrigenous clastic sediments in the base of the island-arc crust. In Chapter 12 it is suggested that some intracontinental plate magmas have high $^{87}Sr/^{86}Sr$ ratios as a consequence of their derivation from Rb/Sr-enriched mantle sources within the subcontinental lithosphere.

The difference in $^{87}Sr/^{86}Sr$ between MORB and OIB suggests that MORB are produced by partial melting of mantle with a significantly lower Rb/Sr ratio than OIB source mantle. This difference must have existed for at least 1–2 Ga to be reflected in the isotopic compositions. It has been suggested (Ch. 5) that MORB are derived by partial melting of a depleted upper mantle layer from which the materials of the continental crust have been progressively extracted throughout the past 4 Ga or so. In contrast, OIB appear to be derived from more enriched mantle sources which may involve primordial mantle components and recycled oceanic and continental lithosphere components (Ch. 9).

Sm–Nd

Samarium and neodymium are light REE, the concentrations of which in igneous rocks increase with increasing degree of differentiation, as they are incompatible. However, the Sm/Nd ratio decreases as Nd is concentrated in the liquid relative to Sm during the course of fractional crystallization. Sm and Nd are joined in a parent–daughter relationship by the alpha decay of ^{147}Sm to stable ^{143}Nd, with a half-life of 106×10^9 years. The decay of ^{147}Sm is described by the equation:

$$\frac{^{143}Nd}{^{144}Nd} = \left(\frac{^{143}Nd}{^{144}Nd}\right)_{initial} + \frac{^{147}Sm}{^{144}Nd}(e^{\lambda t} - 1)$$

where stable ^{144}Nd is used as a reference isotope.

The abundance of radiogenic ^{143}Nd, and hence the $^{143}Nd/^{144}Nd$ ratio of the Earth, has increased with time because of the decay of ^{147}Sm to ^{143}Nd. This can be described by a model based on the age and Sm/Nd ratio of the Earth and its primordial $^{143}Nd/^{144}Nd$ ratio (Fig. 2.9). The latter two parameters are assumed to equal the ratios in chondritic meteorites (referred to as a *Ch*ondritic *U*niform *R*eservoir – CHUR; DePaolo & Wasserburg 1976). Partial melting of a chondritic uniform reservoir increases the Sm/Nd ratio of the residuum, which therefore evolves higher $^{143}Nd/^{144}Nd$ than CHUR. Those parts of the mantle which have not been involved in partial melting events should contain Nd, the isotopic composition of which evolves along the CHUR line in Figure 2.9.

There is still some uncertainty concerning the value of the primordial $^{143}Nd/^{144}Nd$ ratio, caused by differences in analytical procedures between different laboratories (Wasserburg *et al.* 1981). Mea-

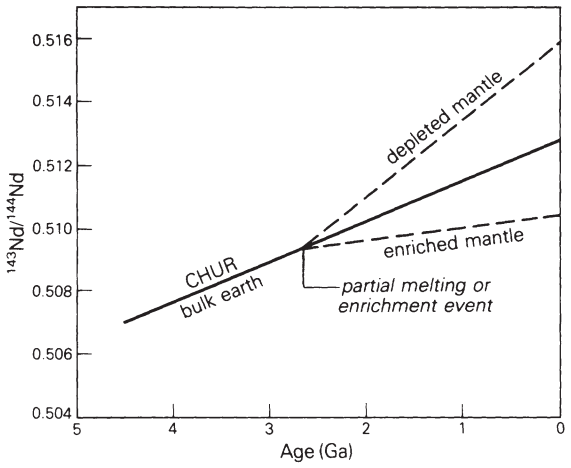

Figure 2.9 Isotopic evolution of Nd in a chondritic uniform reservoir (CHUR). Depleted and enriched mantle reservoirs evolve to higher and lower $^{143}Nd/^{144}Nd$ ratios than CHUR respectively.

sured $^{143}Nd/^{144}Nd$ ratios have been normalized in different ways (Faure 1986). For data corrected to $^{146}Nd/^{142}Nd = 0.636151$, CHUR has $^{143}Nd/^{144}Nd = 0.511847$, whereas for data corrected to $^{146}Nd/^{144}Nd = 0.7219$, the value for CHUR is 0.512638. All Nd isotopic data discussed in Chapters 5–12 have been corrected to the latter value.

To compare differences between the $^{143}Nd/^{144}Nd$ ratios of igneous rocks and CHUR, DePaolo & Wasserburg (1976) introduced the epsilon parameter:

$$\varepsilon_{Nd} = \left[\frac{(^{143}Nd/^{144}Nd)_{\text{initial}}}{I^{t}_{CHUR}} - 1 \right] \times 10^4$$

where I^{t}_{CHUR} is the $^{143}Nd/^{144}Nd$ ratio of CHUR at the time of formation of the rock, t. Calculation of this parameter also circumvents the problem of different inter-laboratory normalization procedures. A positive ϵ value implies that the magmas were formed from depleted mantle, whereas a negative value indicates that they were derived from enriched mantle sources that had a lower Sm/Nd than CHUR.

Combined Nd–Sr

As shown in Figure 2.7a, the $^{143}Nd/^{144}Nd$ and $^{87}Sr/^{86}Sr$ ratios of recent oceanic basalts (MORB and OIB) form a strongly correlated array. This correlation has been used to define an $^{87}Sr/^{86}Sr$ ratio for the bulk Earth complementary to the Nd data. Thus, for a $^{143}Nd/^{144}Nd$ ratio of 0.512638 for CHUR (bulk Earth) at the present time, $^{87}Sr/^{86}Sr$ lies between 0.7045 and 0.7055. In all the Nd–Sr isotope diagrams in Chapters 5–12 a value of 0.7045 has been assumed. The $^{87}Sr/^{86}Sr$ ratio of the bulk Earth derived in this way can be used to define an epsilon parameter analogous to that defined for Nd:

$$\varepsilon_{Sr} = \left[\frac{(^{87}Sr/^{86}Sr)_{\text{initial}}}{(^{87}Sr/^{86}Sr)^{t}_{UR}} - 1 \right] \times 10^4$$

where UR represents 'uniform reservoir', equivalent to bulk Earth. However, in view of the increasing spread of Nd–Sr isotopic compositions being recorded in young volcanic rocks, the bulk earth parameter for the Rb/Sr system should be viewed with caution (White & Hofmann 1982) and most recent articles no longer use the ε_{Sr} notation.

The Nd and Sr isotopic compositions of MORB indicate that they originate from sources that have higher Sm/Nd and lower Rb/Sr than the chondritic reservoir (bulk Earth). Such source regions are said to be depleted, because they appear to have lost Rb and other LIL elements. However, the mantle beneath the ocean basins also appears to contain magma sources which are enriched and have higher Rb/Sr and lower Sm/Nd ratios than bulk Earth.

Typical continental crustal rocks have lower Sm/Nd and therefore lower $^{143}Nd/^{144}Nd$ ratios (negative εNd values) than those derived from the upper mantle (Fig. 2.8). As a consequence, combined Nd–Sr isotopic studies potentially provide a powerful tracer for contamination of magmas by continental crustal rocks.

U–Th–Pb

Uranium has three naturally occurring radioactive isotopes, ^{238}U, ^{235}U and ^{234}U, while Th exists

primarily as one radioactive isotope, ^{232}Th. However, in addition five radioactive isotopes of Th occur in nature as short-lived intermediate daughters of ^{238}U, ^{235}U and ^{232}Th. Pb has four naturally occurring isotopes, ^{208}Pb, ^{207}Pb, ^{206}Pb and ^{204}Pb. Of these, only ^{204}Pb is not radiogenic and is therefore used as a stable reference isotope. ^{238}U, ^{235}U and ^{232}Th are each the parent of a chain of radioactive daughters ending with a stable isotope of Pb:

$$^{238}\text{U} \rightarrow {}^{234}\text{U} \rightarrow {}^{206}\text{Pb}$$

$$^{235}\text{U} \rightarrow {}^{207}\text{Pb}$$

$$^{232}\text{Th} \rightarrow {}^{208}\text{Pb}$$

The isotopic composition of Pb in rocks containing U and Th is given by the following equations:

$$\frac{^{206}\text{Pb}}{^{204}\text{Pb}} = \left(\frac{^{206}\text{Pb}}{^{204}\text{Pb}}\right)_{\text{initial}} + \frac{^{238}\text{U}}{^{204}\text{Pb}}(e^{\lambda_1 t} - 1)$$

$$\frac{^{207}\text{Pb}}{^{204}\text{Pb}} = \left(\frac{^{207}\text{Pb}}{^{204}\text{Pb}}\right)_{\text{initial}} + \frac{^{235}\text{U}}{^{204}\text{Pb}}(e^{\lambda_2 t} - 1)$$

$$\frac{^{208}\text{Pb}}{^{204}\text{Pb}} = \left(\frac{^{208}\text{Pb}}{^{204}\text{Pb}}\right)_{\text{initial}} + \frac{^{232}\text{Th}}{^{204}\text{Pb}}(e^{\lambda_3 t} - 1)$$

The ratio $^{238}\text{U}/^{204}\text{Pb}$ is known as μ.

Following the same logic that we have adopted for the Nd–Sm and Rb–Sr systems, the isotopic composition of Pb at the time of formation of the Earth should be the same as that in meteorites. Chen & Wasserburg (1983) have measured the following isotopic compositions of Pb in troilite (FeS) from the Canyon Diablo iron meteorite, which may be taken to represent the primordial values:

$$\frac{^{206}\text{Pb}}{^{204}\text{Pb}} = 9.3066, \quad \frac{^{207}\text{Pb}}{^{204}\text{Pb}} = 10.293, \quad \frac{^{208}\text{Pb}}{^{204}\text{Pb}} = 29.475$$

Figure 2.10 shows three growth curves for Pb isotopes for typical μ values of 8,9 and 10, assuming that the age of the Earth is 4.55 Ga. These growth curves fan out from the point representing primordial Pb. The straight lines in this diagram are isochrons for ages 0, 1, 2 and 3 Ga. All single-stage leads that were removed from their sources at time t must lie on these isochrons, even if they grew in different source regions (Faure 1986). The line for $t = 0$ is called the *geochron,* and all modern single-stage leads in the Earth and in meteorites must lie on it.

Igneous rocks contain Pb, the isotopic composition of which reflects multistage histories, having evolved in systems with varying U/Pb and Th/Pb ratios for varying lengths of time. Nevertheless, the isotope ratios of cogenetic suites of igneous rocks should define straight lines (isochrons) in plots of $^{206}\text{Pb}/^{204}\text{Pb}$ versus $^{207}\text{Pb}/^{204}\text{Pb}$ or $^{208}\text{Pb}/^{204}\text{Pb}$, similar to those of Figure 2.10, provided that all had the same initial Pb isotopic composition and evolved subsequently with different U/Pb and Th/Pb ratios. However, not all linear arrays on Pb–Pb diagrams need have age significance, as they may also result from mixing of leads of different isotopic composition.

Figure 2.11 shows the variation of $^{207}\text{Pb}/^{204}\text{Pb}$ versus $^{206}\text{Pb}/^{204}\text{Pb}$ for oceanic basalts, subduction-related basalts and intracontinental plate basalts, analogous to Figure 2.7 for Nd–Sr isotopes. The Pb isotopic compositions of MORB and OIB lie to the right of the geochron, defining marked linear arrays, the significance of which remains controversial (Chs 5 & 9). Clearly, the sub-oceanic upper mantle is extremely heterogeneous in terms of its Pb isotopic composition. The Pb isotopic compositions of subduction-related basalts are displaced to the high $^{207}\text{Pb}/^{204}\text{Pb}$ side of the MORB–OIB array (Chs 6 & 7) which, at least for oceanic-island arcs, has been attributed to mixing between mantle Pb and Pb from subducted oceanic sediments. Basalts from intracontinental plate-tectonic settings. (Chs 10–12) display a wide range of $^{207}\text{Pb}/^{204}\text{Pb}$ and $^{206}\text{Pb}/^{204}\text{Pb}$ ratios, which can often be interpreted in terms of crustal contamination of mantle-derived magmas.

U and Th are both preferentially concentrated in

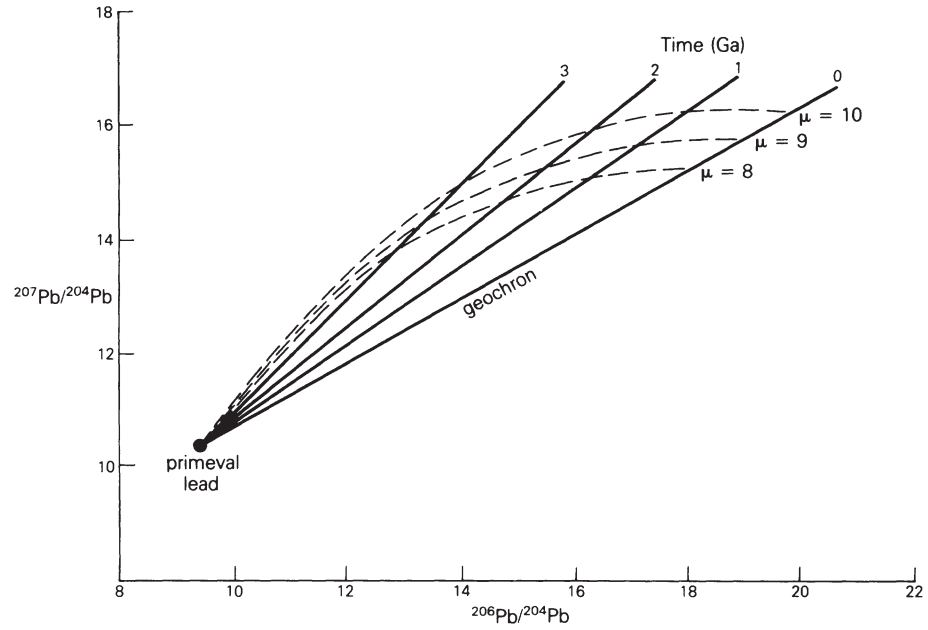

Figure 2.10 Growth curves showing the isotopic evolution of Pb in the Earth. The dashed curved lines are lead growth curves for U–Pb systems having present-day μ values of 8, 9 and 10. The straight solid lines are isochrons for ages 0, 1, 2 and 3 Ga.

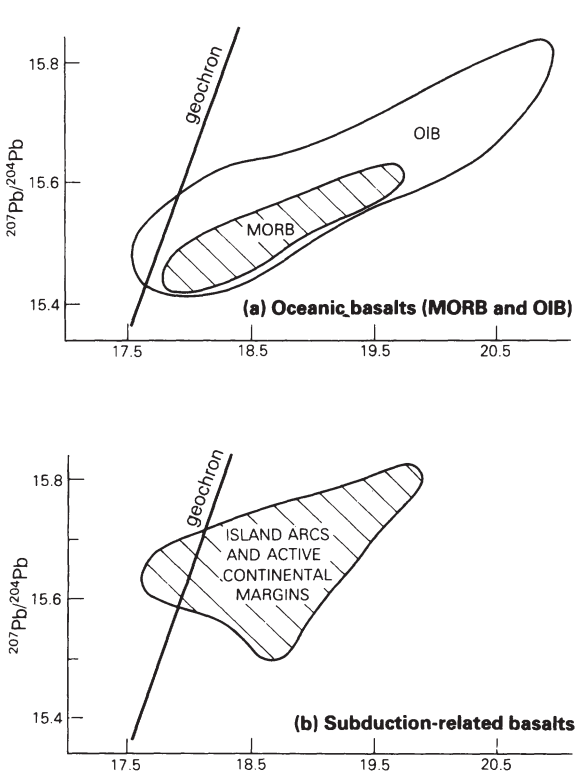

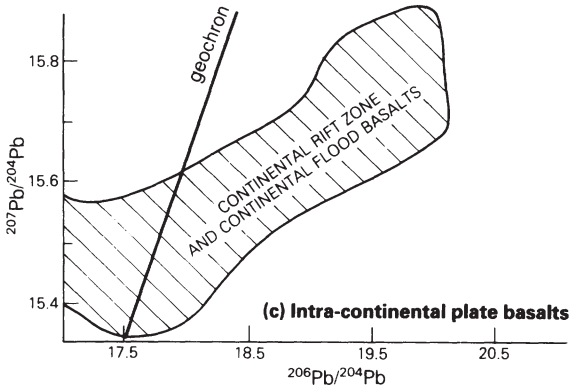

Figure 2.11 Variation of $^{207}Pb/^{204}Pb$ versus $^{206}Pb/^{204}Pb$ for volcanic rocks from different tectonic settings.

silicate melts compared to Pb and, consequently, the U/Pb and Th/Pb ratios of crustal rocks are higher than those of the mantle. Additionally, U and Th are preferentially concentrated in upper crustal rocks and, consequently, the upper and lower crust may have distinctly different Pb isotope signatures (Fig. 2.12). Thus Pb isotopes may provide powerful constraints for the nature of crustal contaminants in continental volcanic suites.

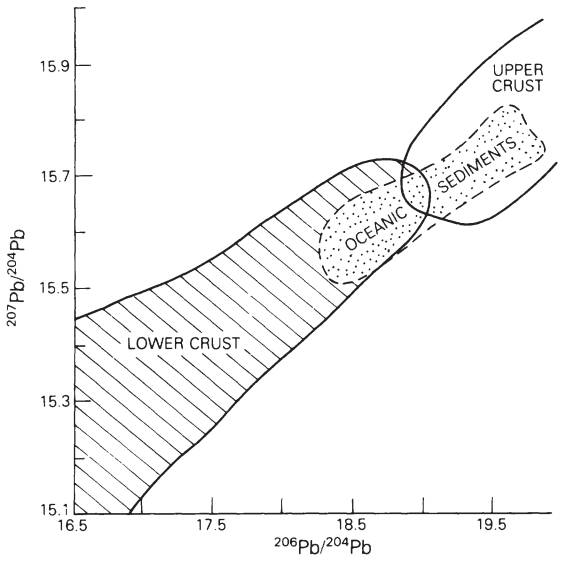

Figure 2.12 Variation of $^{207}Pb/^{204}Pb$ versus $^{206}Pb/^{204}Pb$ for rocks from the upper and lower continental crust. Shown for comparison is the field of oceanic sediments (after Zartman & Doe 1981).

U-series disequilibrium

The decay series arising from ^{238}U and ^{235}U contain radioactive isotopes of many different elements. These daughters of U may be separated from their parents and from each other during partial melting and subsequent fractional crystallization, because of their different geochemical properties. The resulting radioactive disequilibrium may be used for dating over time periods ranging from a few tens of years to one million years (Faure 1986). Additionally, for young volcanic rocks, it may provide useful information concerning the nature of partial melting processes (Ch. 6), and the time elapsed between the initial melting and subsequent extrusion of the lava (Allègre & Condomines 1982). For practical reasons, the abundances of the daughters of U are measured in terms of their activities by means of sensitive radiation detectors.

^{230}Th is a radioactive isotope of Th that is produced in the decay series of ^{238}U. Its immediate parent is ^{234}U and its daughter is ^{226}Ra. The activity of ^{230}Th in young volcanic rocks is described by the following equation (Faure 1986):

$$\left(\frac{^{230}Th}{^{232}Th}\right)_A = \left(\frac{^{230}Th}{^{232}Th}\right)_{Ax} e^{-\lambda_{230}t} + \left(\frac{^{238}U}{^{232}Th}\right)_A (1 - e^{-\lambda_{230}t})$$

where ^{232}Th is used as a reference isotope because of its long half-life (1.4×10^{10} years). The first term describes the decay of unsupported ^{230}Th, while the second term represents the growth of ^{230}Th that is supported by ^{238}U. This is the equation of a straight line in coordinates of $(^{230}Th/^{232}Th)_A$ versus $(^{238}U/^{232}Th)_A$ when t is constant (Fig. 2.13).

At the time of crystallization ($t = 0$), suites of cogenetic volcanic rocks define an isochron with slope equal to zero. Subsequently, the isochron rotates about the equipoint and its slope increases and approaches unity. The isochron with a slope of one is called the *equiline*, and is the locus of points for which $(^{230}Th/^{238}U)_A = 1$, as required by secular equilibrium. The slope of the isochron begins to deviate detectably from zero about 10^3 after crystallization and approaches unity about 10^6 years later. Thus $10^3 - 10^6$ years is the useful range of this geochronometer.

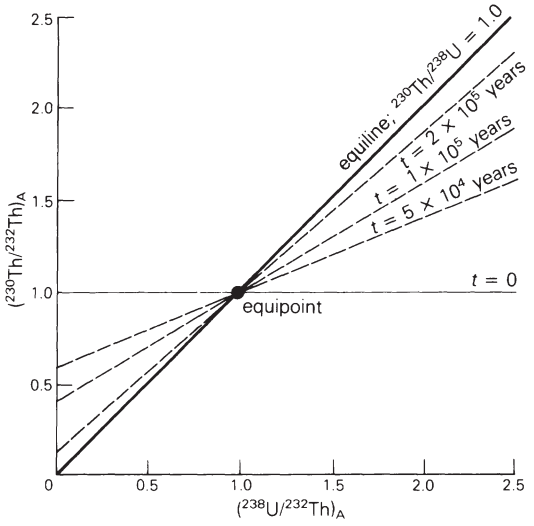

Figure 2.13 $^{230}Th/^{238}U$ isochron diagram (after Faure 1986, Fig. 21.7, p. 379). It should be noted that the $(^{230}Th/^{232}Th)_A$ ratio at $t = 0$ is not constrained to equal unity.

He isotopes

The variation of $^3He/^4He$ in volcanic rocks is due to the balance between primordial He and radiogenic He generated by radioactive decay of ^{232}Th, ^{235}U and ^{238}U. The ratio (R) is generally normalized to the atmospheric value of $^3He/^4He$ (R_a). R/R_a values for OIB range from 1 to 32, whereas MORB define a more restricted range from 5 to 15. Basalts from the oceanic islands of Hawaii and Iceland (Chs 5 & 9) have very high $^3He/^4He$ ratios, which has been considered to reflect the involvement of relatively undegassed (?primordial) mantle components in their petrogenesis (Allègre *et al.* 1986, Zindler & Hart 1986). In contrast, basalts from the oceanic islands of Tristan da Cunha and Gough are characterized by low $^3He/^4He$ ratios of around 5, which may suggest the involvement of recycled source components (Ch. 9).

2.5.2. Cosmogenic radionuclides: ^{10}Be

Cosmogenic radionuclides are produced by the interaction of cosmic rays with atoms in the atmosphere and on the Earth's surface. Be has seven isotopes, the mass numbers of which range from 6 to 12, of which only ^9Be is stable. Unstable ^7Be and ^{10}Be occur in nature because they are produced by nuclear reactions caused by cosmic rays. ^7Be decays to ^7Li with a half-life of 53 days, whereas ^{10}Be has a half-life of 1.5×10^6 years and decays by beta emission to stable ^{10}B.

The cosmogenic Be isotopes are rapidly removed from the atmosphere by precipitation, and are transferred to the sediment at the bottom of the oceans and to the continental ice sheets of Greenland and Antarctica. Their production rates vary with latitude, altitude in the atmosphere and with time. The residence time ($\sim$ 16 years) of ^{10}Be in the surface layer of the oceans is, however, long enough to permit horizontal mixing, which reduces the effect of latitudinal variations in its production rate. Clearly, the abundance of ^{10}Be in a terrestrial reservoir depends upon the production rate, the sedimentation rate and the time elapsed since deposition. High sedimentation rates tend to dilute the concentration of the radionuclide.

The identification of ^{10}Be in some recent subduction-related lavas (Chs 6 & 7) has been used to argue for the role of subducted oceanic sediments in their petrogenesis. However, its absence does not argue against because of its relatively short half-life.

2.5.3 Stable isotopes

Oxygen

Oxygen has three stable isotopes, ^{16}O, ^{17}O and ^{18}O. Its isotopic composition in a sample is generally reported in terms of a parameter $\delta^{18}O$, which is the difference between the $^{18}O/^{16}O$ ratio of the sample and that of a standard called SMOW (*S*tandard *M*ean *O*cean *W*ater):

$$\delta^{18}O = \left[\frac{(^{18}O/^{16}O)_{sample} - (^{18}O/^{16}O)_{SMOW}}{(^{18}O/^{16}O)_{SMOW}}\right] \times 10^3$$

Crystal–liquid fractionation processes during partial melting and subsequent fractional crystallization may potentially cause variations in the oxygen isotope composition of magmas (Kyser *et al.* 1982). However, at magmatic temperatures the mass fractionation of oxygen isotopes is much less pronounced than at atmospheric temperatures and, consequently, the effects are only small (Faure 1986). Thus, broadly speaking, primitive basaltic magmas should have oxygen isotopic compositions which directly reflect those of their mantle source.

Conventionally mantle-derived magmas were considered to have a very narrow range of $\delta^{18}O$ values (from +5.5 to +6‰; James 1981) compared to crustal rock types (Fig.6.47) which have $\delta^{18}O >$ 6. However, Kyser *et al.* (1982) have demonstrated that oceanic basalts actually display a much wider range of $\delta^{18}0$ values (from +4.9 to +8.3‰), which they attribute to oxygen isotope heterogeneity in the mantle source. Nevertheless, oxygen isotopes remain useful indicators of crustal contamination processes because of the contrasting isotopic compositions of continental crustal rocks, which have equilibrated with the hydrosphere, and mantle-derived magmas.

Interaction between crustal material and basic magmas may occur through direct contamination of the magmas as they rise through the continental crust (Chs 7, 10 & 11) or by recycling of crustal materials (sediments) back into the mantle source region of basalts in subduction zones (Chs 6 & 7). Such contamination may involve bulk assimilation of crustal rocks, with resulting elemental mixing of the two reservoirs, or selective elemental or isotopic exchange. In subduction zones the release of fluids or partial melts, from sedimentary rocks and seawater-altered basalt in the subducted ocean crust, into the overlying mantle wedge may be a mechanism for transferring a continental crustal isotopic and trace element signature to the mantle source of the arc basalts.

The isotopic composition of oxygen in young volcanic rocks has been used in conjunction with radiogenic isotopes of Sr, Nd and Pb to detect the contamination of basaltic magmas by crustal rocks. Compared to mantle-derived magmas, the latter are enriched in ^{18}O and radiogenic ^{87}Sr, but depleted in radiogenic ^{143}Nd. As a consequence, addition of O, Sr and Nd from ancient granitic crustal components to basaltic magmas can cause positive correlations between $\delta^{18}O$ and $^{87}Sr/^{86}Sr$ and negative correlations between $\delta^{18}O$ and $^{143}Nd/^{144}Nd$ (e.g. see Ch. 6). However, the shape of the mixing curve may differ significantly depending upon the actual mechanism of contamination (Fig. 6.48), which may be useful in petrogenetic modelling. James (1981), Graham & Harmon (1983) and Faure (1986) have presented useful discussions of the use of stable isotopes in studying the roles of crustal contamination in magmas, and the reader is referred to these works for further details.

2.6 Geochemical criteria for the identification of the palaeotectonic setting of ancient volcanic sequences

Clearly, if we can correlate particular geochemical characteristics of modern volcanic rocks with their specific tectonic setting, we can use these data to identify the tectonic setting of ancient volcanic sequences. However, this approach in itself is unlikely to give an unambiguous determination of the tectonic setting. Instead, we need to consider the overall geological setting of the magmatism (see, e.g., Cas & Wright 1987) including, for example, the nature of the basement and the percentage of pyroclastic rocks within the sequence. The compositions of basaltic magmas are dependent upon their source composition and mineralogy, the depth and degree of partial melting, the mechanism of partial melting and the various fractionation and contamination processes they may have undergone en route to the surface. Only when some or all of these are unique to a particular tectonic setting will we be able to use basalt geochemistry as a diagnostic indicator of tectonic setting.

During the past 15 years, a number of papers have appeared in which the major, minor and trace element compositions of young basaltic rocks have been related to the tectonic environment in which the basalts were generated. These have led to the development of 'tectonomagmatic discrimination diagrams' which may be used to elucidate the tectonic setting of ancient volcanic suites (Pearce & Cann 1973, Floyd & Winchester 1975, Pearce *et al.* 1975, 1977, Wood *et al.* 1979, Shervais 1982, Pearce 1982, Mullen 1983, Meschede 1986). Such discriminant diagrams may be divided into three types (Duncan 1987):

(1) Those which utilize relatively immobile trace and minor elements, the concentration of which can be measured by XRF. The most commonly used are the ternary diagrams Ti/100–Zr–Y.3 (Fig. 2.14; Pearce & Cann 1973) and 2Nb–Zr/4–Y (Fig. 2.15; (Meschede 1986).
(2) Those which use major and minor elements, e.g. TiO_2–K_2O–P_2O_5 and MgO–FeO–Al_2O_3 (Pearce *et al.* 1975, 1977) and TiO_2–MnO–P_2O_5 (Fig. 2.16; Mullen 1983).
(3) Those which use immobile trace elements, the concentrations of which can be determined by INAA. The most commonly used diagrams are the Th–Hf/3–Ta ternary (Fig. 2.17; Wood *et al.* 1979) and Th/Yb versus Ta/Yb (Pearce 1982; e.g. Fig. 7.26).

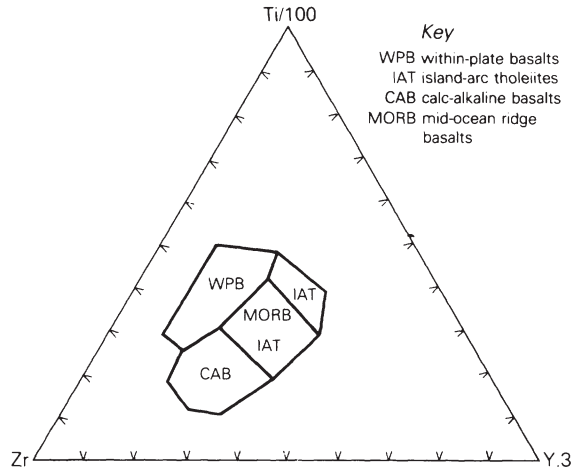

Figure 2.14 Ti/100–Zr–Y.3 tectonomagmatic discrimination diagram for basaltic rocks (after Pearce & Cann 1973, Fig. 3, p. 295).

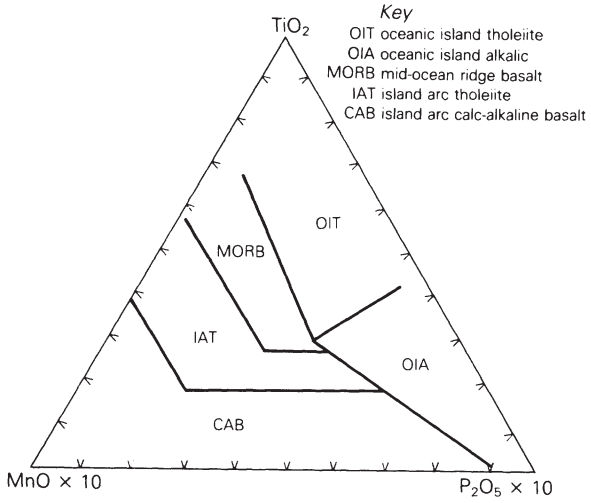

Figure 2.16 TiO_2–MnO–P_2O_5 tectonomagmatic discrimination diagram for oceanic basaltic rocks (after Mullen 1983, Fig. 1, p.54).

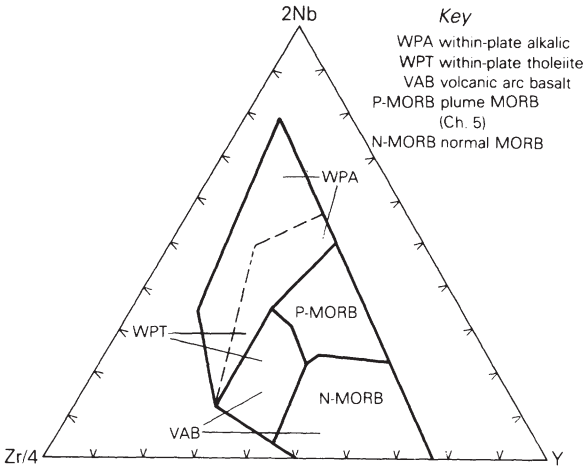

Figure 2.15 2Nb–Zr/4–Y tectonomagmatic discrimination diagram for basaltic rocks (after Meschede 1986, Fig. 1, p. 211).

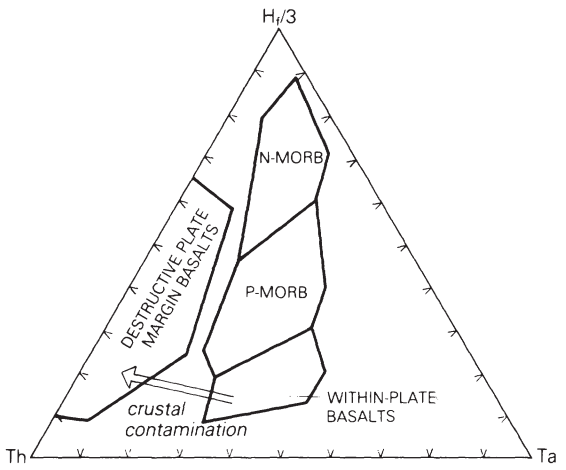

Figure 2.17 Hf/3–Th–Ta tectonomagmatic discrimination diagram for basalts and more differentiated rocks (after Wood *et al.* 1979a, Fig. 3, p. 332.

In order to use these diagrams (except that of Wood *et al.* shown in Fig. 2.17), it is necessary to know the degree of fractionation of the volcanic rock being classified, as they are only strictly applicable to basic volcanic rocks. However, this is not always apparent from the major element chemistry after the rock has been weathered or metamorphosed.

On the whole, major element geochemistry is not particularly useful for tectonomagmatic discrimination. Nevertheless, as we can see from Table 1.3, specific magma types are associated with particular tectonic settings, for example the association of calc-alkaline magmas with subduction zones. It is uncertain whether these discriminant diagrams are

valid for very old rocks, as magma genesis in the Precambrian may have been very different from that of today. In particular, the Precambrian mantle would have experienced fewer melting episodes and would therefore be richer in incompatible elements.

Using the above types of discriminant diagrams it is found that, in general, the correct identification of tectonic setting is highest for magmas not erupted in within-continental-plate environments. Unfortunately, this is precisely the environment in which volcanic rocks are most easily preserved. In general, relatively few continental flood basalt data sets were used to establish the discriminant boundaries, and several recent papers (Holm 1982, Prestvik & Goles 1985, Duncan 1987, Marsh 1987) have noted that some continental flood basalts (CFBs) do not plot in the within-plate fields. However, this does not necessarily invalidate the diagrams for, as we shall see in Chapter 10, CFBs may actually be generated in a variety of tectonic settings. Many clearly have mixed geochemical characteristics; for example, features of both intraplate and subduction-related tectonic settings.

For a combination of elements to be useful in characterizing magma types from different tectonic settings they must ideally have a much greater variation in concentration between samples from different environments than between samples from the same environment. Also, the trace element classification employed should distinguish as many different environments as possible. Clearly, to be of any value in determining the palaeotectonic setting of altered volcanic rocks the selected trace elements must be immobile, i.e. they must not be transported significantly in the fluid phase during weathering and metamorphism. Elements such as Na, K, Ca, Ba, Rb and Sr, and possibly the light REE, are mobile and therefore are not useful for tectonomagmatic discrimination purposes. Thus we cannot in general use the alkali-silica diagram (Fig. 1.1) to reliably classify the volcanic rocks of ancient sequences. In contrast, elements such as Fe, Ti, Ni, Cr, V, Zr, Nb, Ta and Hf may be relatively immobile. The establishment of which element to use is clearly an empirical process, and problems frequently arise because elements which are immobile during weathering may become mobile during the lower grades of metamorphism.

In addition to these simple discriminant diagrams, it is possible to compare a much wider range of trace elements in basalts from known and unknown tectonic settings using normalized trace element variation diagrams or spiderdiagrams (Section 2.3.2). A similar approach has been used in Chapter 10 in which, instead of normalizing to chondritic or primordial mantle abundances, we normalize to the composition of a basalt type generated in a known tectonic setting, e.g. MORB or oceanic-island tholeiite. The problem then becomes one of choosing an average composition to define the normalizing constants which may be considered typical of a particular magma generation environment. Pearce (1987) has developed a computerized system for the identification of the eruptive setting of ancient volcanic rocks, based on this approach, which integrates geological, petrological, mineralogical and geochemical data.

On the basis of the geochemical data presented in Chapters 5–12 it is clear that particular trace element abundance patterns (spiderdiagrams) and Sr–Nd–Pb isotopic signatures are associated with different magma generation environments. However, in many provinces there is still some controversy concerning the detailed petrogenetic interpretation of these data. Additionally, there are clearly some geochemical signatures which are not necessarily unique to a single tectonic environment (Arculus 1987, Duncan 1987). For example, the trace element characteristics of subduction-related basalts are rather similar to those of intracontinental plate basalts which have become contaminated by the continental crust.

Further Reading

Cox, K. G., J. D. Bell & R. J. Pankhurst 1979. *The interpretation of igneous rocks*, London: Allen and Unwin; Ch. 2.

Faure, G. 1986. *Principles of isotope geology*, 2nd edn New York: John Wiley

Graham, C. M. & R. S. Harmon 1983. Stable isotope evidence on the nature of crust-mantle interactions. In *Continental basalts and mantle*

xenoliths, C. J. Hawkesworth & M. J. Norry (eds), 20–45. Nantwich: Shiva.

Hanson, G. N. 1980. Rare earth elements in petrogenetic studies of igneous systems. *Ann. Rev. Earth Planet. Sci.* **8**, 371–406.

James, D. E. 1981. The combined use of oxygen and radiogenic isotopes as indicators of crustal contamination. *Ann. Rev. Earth Planet. Sci.* **9**, 311–44.

Potts, P. J. 1987. *A handbook of silicate rock analysis*. London: Blackie.

Thompson, R. N., M. A. Morrison, G. L. Hendry & S. J. Parry 1984. An assessment of the relative roles of crust and mantle in magma genesis. *Phil Trans R. Soc. Lond.* **A310**, 549–90.